THE SHELL-MODEL POTENTIAL FROM A RELATIVISTIC HARTREE-FOCK APPROACH

(13)

M. Jaminon, C. Mahaux and P. Rochus
Institut de Physique, Université de Liège, Belgium.

SUMMARY. A model relativistic quantum field theory is used to calculate the average binding energy per nucleon and, mainly, the single-particle nuclear potential at low and at intermediate energy. We consider the interaction of the nucleon field with effective scalar and vector meson fields. We limit ourselves to lowest order, i.e. to the Hartree-Fock approximation. We construct a non-relativistic local shell-model potential which yields exactly the same elastic scattering phase shifts and bound state energies as the relativistic single-particle potential. The comparison of this shell-model potential with empirical data is satisfactory provided that the coupling strengths between the nucleon and the meson fields are suitably chosen. The wine-bottle bottom shape that we had previously found in the framework of the Hartree approximation for the single-particle potential at intermediate energy is maintained when the Fock contribution is included.

International School of Physics "Enrico Fermi"
Varenna 1980 ITALY

1.- INTRODUCTION

Walecka [1] and collaborators [2,3] have recently developed a model relativistic quantum field theory of nuclear matter and of finite nuclei. In the simplest and most investigated form of this model, the nucleon field interacts with a neutral scalar meson (σ) field and with a neutral vector meson (ω) field. Although this is a daring over-simplification of the nuclear Lagrangian, the model deserves detailed scrutiny not only because it yields fair agreement with a number of experimental data, but mainly because it includes some mesonic degrees of freedom in a way which is completely consistent with the requirements of relativistic quantum field theory. All equations therefore appear in a Lorentz covariant form. In particular, it is natural that in this approach the single-particle wave equation of the shell-model emerges in the form of the relativistic Dirac equation rather than in the form of the non-relativistic Schroedinger equation. The present paper is mainly devoted to this relativistic single-particle wave equation, and to its relationship with the familiar non-relativistic shell-model potential. More specifically, our main purpose is twofold : (i) We discuss the relativistic Hartree-Fock approximation. While the Hartree approximation has already been investigated in some detail in the available literature [4-7], the Fock contribution had never been properly investigated. (ii) We construct a local single-particle potential which can be introduced in the Schroedinger equation and then yields exactly the same phase shift and bound state energies as those which would be obtained from the relativistic wave equation. This step is largely independent of the (e.g. Hartree or Hartree-Fock) approximation which has led to a relativistic wave equation, whence its intrinsic interest.

The main features of the relativistic quantum field model are briefly described in Section II. The Hartree and the Hartree-Fock approximations are investigated in Sections III and IV, respectively. In Section V, we discuss some limitations and possible extensions of our work. In many instances we write the equations only in the limit of infinite nuclear matter, in which they take a simpler and more transparent form.

II.- THE RELATIVISTIC QUANTUM FIELD MODEL

Following Walecka [1] and others [4,5], we adopt the following Lagrangian density

$$(1) \qquad L = L_N^{free} + L_\sigma^{free} + L_\omega^{free} + L_{\sigma N}^{int} + L_{\omega N}^{int} \quad ,$$

where the last two terms respectively describe the interaction between the nucleon N on the one hand, and the scalar meson σ and the vector meson ω on the other hand. The relativistic single-particle potential can be identified with the self-energy operator. The most systematic calculational procedure probably consists in expanding the self-energy in powers of the strength of the meson-nucleon interaction [8]. Alternative methods exist, see e.g. refs. [1] and [9]. These methods are largely equivalent in the the Hartree approximation. Here, it is convenient to adopt the presentation of Miller and Green [4] and of Brockmann [5], to whom we refer for further detail. These authors treat the meson fields as classical fields ; this implies the omission of all quantities containing annihilation or creation operators for antiparticles and renders this approach inappropriate for going beyond the Hartree-Fock approximation in a systematic way. They obtain the following nuclear Hamiltonian

$$(2) \qquad H = \sum_{\alpha,\alpha'} \int d^3x \; f_\alpha^\dagger,(\underline{x}) \; \gamma_0(-i\underline{\gamma}\cdot\underline{\nabla}+m) \; f_{\alpha'}(\underline{x}) \; b_\alpha^\dagger, \; b_{\alpha'} +$$

$$\frac{1}{2} \sum_{\substack{\alpha,\alpha' \\ \delta,\delta'}} \int d^3x_1 \; d^3x_2 \; f_\alpha^\dagger,(\underline{x}_1) \; f_\delta^\dagger,(\underline{x}_2) \; V^{\alpha\alpha'}(|\underline{x}_1-\underline{x}_2|)$$

$$f_{\delta'}(\underline{x}_2) \; f_{\alpha'}(\underline{x}_1) \; b_\alpha^\dagger, \; b_\delta^\dagger, \; b_{\delta'} \; b_{\alpha'} \quad .$$

Here, $\{f_\alpha(\underline{x})\}$ is a complete set of Dirac spinors and b_α (resp. $b_\alpha^\dagger$) denotes an annihilation (resp. a creation) operator for a nucleon in state α . The nucleon-nucleon interaction in Equation (2) reads

$$(3) \qquad V^{\alpha\alpha'}(|\underline{x}_1-\underline{x}_2|) = \sum_{i=\sigma,\omega} \Gamma_i(1,2) \; V_i^{\alpha\alpha'}(|\underline{x}_1-\underline{x}_2|) \quad ,$$

with

$$(4) \qquad \Gamma_\sigma(1,2) = -\gamma_\sigma(1) \; \gamma^0(2) \quad ,$$

$$(5) \qquad \Gamma_\omega(1,2) = \gamma_0(1) \; \gamma^0(2) \; \gamma_\mu(1) \; \gamma^\mu(2) \quad ,$$

$$(6) \qquad V_i^{\alpha\alpha'}(r) = \frac{g_i^2}{4\pi} \frac{\Lambda_i^2}{\Lambda_i^2-m_i^2} \frac{1}{r} \{\exp(-r[m_i^2 - (E_\alpha - E_{\alpha'})^2]) - \exp(-r[\Lambda_i^2 - (E_\alpha - E_{\alpha'})^2])\} \quad ,$$

where Λ_i is a cut-off momentum and m_i is the mass of meson i , while E_α denotes the relativistic total energy of a nucleon in state α .

3.- HARTREE APPROXIMATION

3'1. Relativistic form

The Hartree approximation for the single-particle potential can be derived from the model Hamiltonian (2) in the usual way [4,5]. It is a local and energy independent operator. In a doubly-magic nucleus, the corresponding relativistic single-particle wave equation reads

$$(7) \qquad \{\underline{\alpha}\cdot\underline{p} + \gamma_0[m + U_s^H(r) + \gamma_0 \; U_0^H(r)]\} \; \psi_q(\underline{r}) = E_q \; \psi_q(\underline{r})$$

where the upper index H refers to "Hartree" and the lower index q labels the eigenstates. The scalar and the vector relativistic single-particle potentials are given by

$$U_s^H(r) = -\int d^3r'\ \rho_s(r')\ V_\sigma^{aa}(|\underline{r}-\underline{r}'|) \quad , \tag{8}$$

$$U_o^H(r) = \int d^3r'\ \rho(r')\ V_\omega^{aa}(|\underline{r}-\underline{r}'|) \quad . \tag{9}$$

Here, $\rho(r)$ and $\rho_s(r)$ are the baryon density and the self-consistent scalar density, respectively :

$$\rho(r) = \sum_{q=1}^{A} \psi_q^+(\underline{r})\ \psi_q(\underline{r}) \quad , \tag{10}$$

$$\rho_s(r) = \sum_{q=1}^{A} \bar{\psi}_q(\underline{r})\ \psi_q(\underline{r}) \quad . \tag{11}$$

The sums in Equations (10) and (11) run over the A lowest occupied eigenstates.

These relations take a simple form in the case of nuclear matter. If k_F denotes the Fermi momentum, one then finds [7]

$$U_o^H = \frac{g_\omega^2}{m_\omega^2}\,\rho \quad , \qquad U_s^H = -\frac{g_\sigma^2}{m_\sigma^2}\,\rho_s \quad , \tag{12}$$

$$\rho = \frac{2}{3\pi^2}\,k_F^3 \quad , \qquad \rho_s = \frac{4}{(2\pi)^3}\int_0^{k_F} d^3k\ \frac{m^*}{[k^2+m^{*2}]^{\frac{1}{2}}} \tag{13}$$

where

$$m^* = m + U_s^H \tag{14}$$

is the "effective mass". In the Hartree approximation, the average binding energy per nucleon is given by

$$\frac{B}{A} = \sum_{k<k_F} [T(k) + \tfrac{1}{2}\,\Sigma(k)] \quad , \tag{15}$$

where

$$T(k) = \langle \psi_{\underline{k}} | \gamma_0 (\underline{\gamma}\cdot\underline{k}+m) | \psi_{\underline{k}} \rangle - m \quad , \tag{16}$$

and

$$\Sigma(k) = \langle \psi_{\underline{k}} | U_o^H + \gamma_o\, U_s^H | \psi_{\underline{k}} \rangle \tag{17}$$

denote the relativistic kinetic energy and the potential energy, respectively, of a nucleon with momentum $\underline{k}$.

The results presented below have been obtained from the following parameter values

$$g_\sigma^2/4\pi = 6.57 \quad , \qquad m_\sigma = 550\ \text{MeV} \quad , \tag{18a}$$

$$g_\omega^2/4\pi = 9.25 \quad , \qquad m_\omega = 782.8\ \text{MeV} \quad , \tag{18b}$$

and with a cut-off form factor characterized by a mass $\Lambda = 1530$ MeV . These are the values which had been adopted by Brockmann [5] in his self-consistent relativistic Hartree calculation of the ground states of ^{16}O and of ^{40}Ca . They are identical to the σ- and ω-meson parameters of the one-boson-exchange potential (OBEP) of the Bonn group [10]. We emphasize, however, that the latter property does not imply that this particular choice has any "fundamental" implication. Indeed, the Bonn OBEP contains a number of components which are omitted here and correspond to the exchange of other mesons (π, ρ, ...). Moreover, there certainly exist sizeable corrections to the Hartree approximation, due to the Fock term (Section IV) and to higher order diagrams [8,11]. In general, the input meson parameters of a Hartree or of a Hartree-Fock calculation should therefore be considered as <u>effective</u> coupling constants and masses [1]. We return to this point in Section V.

The full curve in fig. 1 represents the average binding energy per nucleon as calculated from the Hartree approximation (15). We note that at saturation the calculated Fermi momentum ($k_F = 1.51\ \text{fm}^{-1}$) and the calculated average binding energy per nucleon ($B/A = -21.6$ MeV) are both larger than the empirical values ($k_F = 1.36\ \text{fm}^{-1}$, $B/A = -16$ MeV) . This indicates, in particular, that in finite nuclei the root mean square radius of the density distribution as calculated from this relativistic Hartree model will be somewhat too small.

This is confirmed by Brockmann's calculation [5]. It can be checked that Equations (12)-(17) are identical to those derived by Walecka [1] in the framework of his "mean field approximation". They differ from the direct part of the lowest order contribution to the self-energy [8] by the fact that here the effective mass m^* has to be calculated self-consistently from Equations (12)-(14). Correspondingly, the spinor ψ_k in Equation (17) does not describe a free plane wave but it instead includes the effect of the Hartree potential $U_s^H + \gamma_o U_o^H$. It appears that this self-consistent requirement has been neglected in ref. [11]. We also note that the baryon density ρ differs from the scalar density ρ_s, see Equations (13). Figure 2 shows that this difference increases with increasing Fermi momentum. This has the effect of increasing the density at saturation as compared to the value that it would take if one would set $\rho_s = \rho$.

3'2. Non-relativistic form

In the case of finite nuclei, one possible test of the relativistic Hartree approximation consists in comparing with experiment the bound single-particle energies E_k and the baryon density distribution $\rho(r)$ calculated from the self-consistent set of equations (7)-(11) [4,5]. However, one can perform a more severe test. Indeed, the accumulation of data on bound and, mainly, scattering states of many nuclei have led to a very good knowledge of the shell-model potential. In its practical formulation, the latter is a local, energy-dependent operator which, when substituted in the non-relativistic Schroedinger equation, yields the experimental single-particle energies and, if supplemented by an imaginary component, the experimental elastic scattering phase shifts. Hence, it is useful to construct here a potential which, when inserted in a Schroedinger equation, yields the same bound state energies and the same elastic scattering phase shifts as those which would be obtained from the relativistic Dirac Equation (7). We dub this potential the "Schroedinger equivalent potential" and we denote it by $U_e(r;\varepsilon)$ where $E = \varepsilon + m$. Its construction proceeds as follows.

Let us denote by $G(r;\varepsilon)$ the radial part of the large components of the relativistic single-particle wave function $\psi_q(r)$. It can easily be shown [5] that the quantity

$$g(r;\varepsilon) = [D(r;\varepsilon)]^{-\frac{1}{2}} G(r;\varepsilon) \quad , \tag{19}$$

with

$$D(r;\varepsilon) = \varepsilon + 2m + U_s^H(r) - U_o^H(r) \tag{20}$$

fulfils the following Schroedinger-like radial wave equation [7]

$$\frac{d^2 g(r;\varepsilon)}{dr^2} + \{k_\infty^2 - \frac{\ell(\ell+1)}{r^2} - 2m\,[U_e(r;\varepsilon) + \frac{1}{r} U_{so}(r;\varepsilon)\,\sigma.L]\} \tag{21}$$

$$g_k(r;\varepsilon) = 0 \quad ,$$

where k_∞ denotes the relativistic momentum at large distance

$$k_\infty^2 = 2\,m\,\varepsilon + \varepsilon^2 \quad , \tag{22}$$

while

$$U_e(r;\varepsilon) \approx U_s(r) + U_o(r) + (2m)^{-1}\,[U_s^2(r) - U_o^2(r)] + \frac{\varepsilon}{m} U_o(r) \quad , \tag{23}$$

$$U_{so}(r;\varepsilon) = -\,[2m\,D(r;\varepsilon)]^{-1} \frac{d}{dr}\,[U_s(r) - U_o(r)] \quad . \tag{24}$$

Here and in the following we usually drop the upper index H, for simplicity. In Equation (23), the sign $\approx$ refers to the omission of negligible surface terms. We note that U_e depends on energy and that the Schroedinger-equivalent potential contains a spin-orbit component.

The quantities $U_e(r;\varepsilon)$ and $U_{so}(r;\varepsilon)$ can be compared with the central and spin-orbit components of the empirical shell-model potential. The quantity which is best determined

by the experimental data is the volume integral per nucleon

$$(25) \qquad J_{U_e}/A = A^{-1} \int d^3r \, U_e(r;\varepsilon) \quad .$$

Figure 3 shows that in the case of ^{40}Ca the calculated and empirical values of this quantity are in good agreement over a wide energy range. The same holds in the case of ^{16}O [6]. The calculated and empirical values of the spin-orbit component $U_{so}(r;\varepsilon)$ are also in fair agreement [7].

We now turn to a brief discussion of the meaningfulness of these agreements. The model contains two main parameters, namely the strengths U_o and U_s of the vector and of the scalar potentials at the Fermi momentum $k_F = 1.35$ fm^{-1} which corresponds to the central density of nuclei. The theoretical potential depth U_e is energy-dependent, with a slope given by U_o/m (see Equation (26) below). Since the empirical value of this slope is approximately equal to 0.3, the value of U_o must be approximately equal to $+ 300$ MeV. Since moreover the depth U_e at low energy is approximately equal to $- 55$ MeV, one must have $U_s = - 350$ MeV. This shows that the model parameters can always be chosen in such a way that U_e is in fair agreement with experiment at low and intermediate energy. Then, however, no parameter is left : U_{so} is uniquely predicted by the model ; the fair agreement between the empirical and experimental values of $U_{so}(r;\varepsilon)$ is therefore by no means a trivial consequence of the choice of the input parameters.

Another noticeable and unavoidable feature of the present model is that U_o and U_s are comparable in magnitude to the nucleon rest mass. Hence, it appears that a relativistic approach is not a luxury. Indeed, it is then quite difficult to derive a Schroedinger equation as an accurate non-relativistic limit of the Dirac Equation (7). In particular, the Foldy-Wouthuysen transformation is not very useful [7]. We emphasize that the Schroedinger-like equation (21) is exact in the sense that the eigenvalues calculated from Equation (21) are the same as those of Equation (7) and that the asymptotic

behaviour of $g(r;\varepsilon)$ for large r is the same as that of $G(r;\varepsilon)$. In order to complete the proof that it is legitimate to identify $U_e(r;\varepsilon)$ with the standard non-relativistic optical-model potential, one must still show that the differential elastic scattering and polarisation cross sections can be obtained in the same way from Equation (21) as from the usual phase shift formula associated with the Schroedinger equation. This can be checked by comparing the equations contained in refs. [12] and [13].

3'3. Wine-bottle bottom shape

In infinite nuclear matter, the Schroedinger-equivalent potential reads

$$(26) \qquad U_e(\varepsilon) = U_s + U_o + (2m)^{-1} [U_s^2 - U_o^2] + \frac{\varepsilon}{m} U_o \quad ,$$

where U_o and U_s are given by Equations (12) in the case of the Hartree approximation. This quantity is plotted in fig. 4 for two values of the Fermi momentum, namely $k_F = 1.35$ fm^{-1}, which corresponds to the nuclear interior, and $k_F = 1.10$ fm^{-1}, which corresponds to the nuclear surface. We note that the two curves intersect. This indicates that in a finite nucleus the Schroedinger-equivalent potential is still attractive at the nuclear surface at the energy at which it becomes repulsive in the nuclear interior. This "wine-bottle bottom shape" is exhibited in fig. 5. Its origin has been discussed in refs. [6,7]. It mainly lies in the quadratic term $(2m)^{-1} [U_s^2 - U_o^2]$ in Equation (23). This quadratic term is characteristic of the relativistic Dirac approach, and of the scalar and vector nature of U_s and of $\gamma_o U_o$, respectively. Early empirical evidence for a wine-bottle bottom shape was claimed by Elton [14] who fitted polarization, reaction and elastic scattering data for 180 MeV protons on ^{56}Fe. In fig. 6 we show that Elton's phenomenological potential is in fair agreement with the Schroedinger-equivalent potential as calculated from our nuclear matter results by means of a local density approximation. Recent

analyses of the scattering of 181 MeV protons by ^{40}Ca [15] and of 200 MeV protons by ^{12}C and ^{13}C [16] corroborate the existence of a wine-bottle bottom shape for the real part of the optical-model potential. We note that this shape has also been found in a theoretical calculation performed in the framework of the Brueckner-Hartree-Fock approximation based on Reid's hard core nucleon-nucleon interaction [17]. However, the interpretation of the phenomenon appears to be quite different in the latter theoretical model, in which it is due to Pauli and binding corrections [18].

4.- HARTREE-FOCK APPROXIMATION

4·1. Schroedinger-equivalent potential in nuclear matter

In the relativistic Hartree-Fock approximation, the single-particle potential contains non-local terms, as in the familiar non-relativistic case. In other words, the left-hand-side of the relativistic Dirac single-particle wave Equation (7) now contains an additional term of the form

$$(27) \qquad \gamma_o \int d^3r'\, U^{NL}(\underline{r},\underline{r}')\, \psi_q(\underline{r}') \quad ,$$

where the upper index NL refers to "non-local", and where U^{NL} in general contains several components which transform as Lorentz-scalar, -vector,-pseudoscalar,... quantities, respectively, if several types of mesons are considered [19]. In order to keep the discussion simple, it is advantageous to consider the case of infinite nuclear matter. Then, $U^{NL}(\underline{r},\underline{r}')$ is a function of $|\underline{r}-\underline{r}'|$ only, while

$$(28) \qquad \psi_{\underline{k}}(\underline{r}) = u(\underline{k}) \exp(i\, \underline{k}.\underline{r}) \quad ,$$

where $u(\underline{k})$ is a four component spinor. It is then appropriate to use the momentum representation. It can be shown [8] that

one can write the Fourier transform of $U^{NL}(|\underline{r}-\underline{r}'|)$ in the form

$$(29) \qquad U^{NL}(\underline{k}) = U_s^{NL}(k) + \gamma_o\, U_o^{NL}(k) + \gamma_o\, \underline{\alpha}.\frac{\underline{k}}{k}\, U_v^{NL}(k) \quad ,$$

where the quantities U_s^{NL} , U_o^{NL} and U_v^{NL} are scalar functions of k , rather than matrices.

The form (29) is of course also valid for the local part, or equivalently for the momentum independent part, of the single-particle potential. We thus temporarily drop the upper index "NL" . The relativistic single-particle wave equation reads

$$(30) \qquad (\underline{\alpha}.\underline{k} + \gamma_o[m + U_s(k) + \gamma_o\, U_o(k) + \gamma_o\, \underline{\alpha}.\frac{\underline{k}}{k}\, U_v(k)])u(\underline{k}) = E_k\, u(\underline{k}) \quad .$$

In order to obtain a Schroedinger-equivalent potential, we proceed as in Section 3·2. We thus eliminate the small components of $u(\underline{k})$ and obtain the following dispersion relation ($E_k = \varepsilon_k + m$) :

$$(31) \qquad \frac{k^2}{2m} + U_s(k,\varepsilon) = \varepsilon + \frac{\varepsilon^2}{2m} = k_m^2 \quad ,$$

with

$$(32) \qquad U_s(k,\varepsilon) = U_o(k) + U_s(k) + (2m)^{-1}\,[U_s^2(k) - U_o^2(k) + U_v^2(k)]$$
$$+ \frac{\varepsilon}{m}\, U_o(k) + \frac{k}{m}\, U_v(k) \quad ,$$

where k and ε are related to one another by Equation (31). By comparing this result with Equation (26), we note that since all quantities now depend on the momentum k one can probably not infer accurate information on each of these various quantities from our knowledge of the energy dependence of the depth of the empirical optical-model potential. One must thus turn to dynamical models. In the next Section, we briefly discuss the Hartree-Fock approximation in the case of the σ,ω model.

4·2. Hartree-Fock approximation

We restrict the present discussion to the case of infinite nuclear matter and to the σ,ω model. We only state some results. A detailed discussion will be published elsewhere. In keeping with the general expressions given in Section 4·1, the Hartree-Fock approximation yields the following relativistic single-particle wave equation

$$(33)\quad \{\underline{\alpha}\cdot\underline{k} + \gamma_o\,[m + U_s^N + \gamma_o\,U_o^H + U^F(\underline{k})]\}\,u(\underline{k}) = E_k\,u(\underline{k}) \quad ,$$

with

$$(34)\quad U^F(\underline{k}) = U_s^F(k) + \gamma_o\,U_o^F(k) + \gamma_o\,\underline{\alpha}\cdot\frac{\underline{k}}{k}\,U_v^F(k) \quad .$$

The quantities U_o^H and U_s^H are still given by Equations (12). However, the expression of ρ_s which was given by Equation (13) in the Hartree approximation is now modified by the fact that the spinor $u(\underline{k})$ contains the influence of $U^F(k)$: one has

$$(35)\quad \rho_s = \frac{4}{(2\pi)^3}\int_o^{k_F} d^3k\,\frac{\bar{m}(k)}{[k_v^2 + \bar{m}^2(k)]^{\frac{1}{2}}}$$

where the momentum-dependent "effective mass" $\bar{m}(k)$ reads

$$(36)\quad \bar{m}(k) = m + U_s^H + U_s^F(k)$$

while

$$(37)\quad k_v = k + U_v^F(k) \quad .$$

The expressions of $U_s^F(k)$, $U_o^F(k)$ and $U_v^F(k)$ will not be given here. They are similar to results given in refs. [8,20] with, however, some complications due to the fact that here we calculate $u(\underline{k})$ self-consistently rather than taking a free plane-wave spinor. One striking difference with the Hartree approximation is that the σ- and the ω-mesons both contribute to all three terms $U_s^F(k)$, $U_o^F(k)$ and $U_v^F(k)$.

It turns out that the contribution of $U_v^F(k)$ to the expression (32) of the Schroedinger-equivalent potential is rather negligible. For low k , the attractive quantity $U_s^F(k)$ is equal to about 25 per cent of the Hartree component U_s^H of the scalar potential ; it tends towards zero for large k . For low k , the repulsive quantity $U_o^F(k)$ is equal to approximately forty per cent of the Hartree contribution U_o^H to the fourth component of the vector potential. The Schroedinger-equivalent potential $U_e^{HF}(\varepsilon)$ (fig. 7) that corresponds to the relativistic Hartree-Fock approximation in the σ,ω model is thus less attractive than the Schroedinger-equivalent potential associated with the relativistic Hartree approximation. Hence, the fair agreement with the empirical shell-model potential depth which had been found in the case of the relativistic Hartree approximation no longer holds for the Hartree-Fock approximation if one adopts the input parameters (18). Clearly, however, it is possible to somewhat increase the strength g_o^2 of the coupling between the scalar and the nucleon fields in order to obtain a good agreement between the Hartree-Fock approximation and the empirical data. This increase would be legitimate since we emphasized in Section 3·1 that the input parameters should be considered as "effective" coupling constants. We find it remarkable that the modification which is required is rather small. We also note that the two curves in fig. 7 intersect, as was also the case in fig. 4. This shows that the relativistic Hartree-Fock maintains a wine-bottle bottom shape for the Schroedinger-equivalent potential at intermediate energy. In turn, this reflects the fact that the momentum dependence of $U_o^F(k)$ and of $U_s^F(k)$ is quite weak because in the present model the effective nucleon-nucleon interaction has short range.

In the self-consistent relativistic Hartree-Fock approximation, the average binding energy per nucleon is given by

$$(38)\quad \frac{B}{A} + m = \frac{3}{k_F^3}\int_o^{k_F} k^2dk\,\{\tfrac{1}{2}\,U_o(k) + \tfrac{1}{2}\,[U_s(k)\,\bar{m}(k) + k_vU_v(k)]\,[k_v^2 + \bar{m}^2(k)]^{-\frac{1}{2}} + [m\,\bar{m}(k) + k_vk][k_v^2 + \bar{m}^2(k)]^{-\frac{1}{2}}\} \quad .$$

The quantity B/A as calculated from this approximation is represented by the dashed curve in fig. 1. As expected from the preceding discussion, it is less attractive than the Hartree-Fock approximation. Saturation is reached for $k_F = 1.36\ fm^{-1}$, where $B/A = -8.6$ MeV.

5.- DISCUSSION

The present contribution is centered on the belief that a formulation of the shell model in the framework of relativistic quantum field theory will lead to a relativistic Dirac single-particle wave equation rather than to a non-relativistic Schroedinger single-particle wave equation. In the non-relativistic approach, the shell model emerges from the Hartree-Fock approximation, in which the effective nucleon-nucleon interaction is in practice either adjusted in a purely phenomenological way or else is estimated from realistic nucleon-nucleon potentials via some (e.g. Brueckner) approximation scheme. Likewise, we considered here the shell-model potential in the framework of a relativistic Hartree-Fock approximation. We adopted a simple model in which the interaction between two nucleons is mediated by the exchange of a scalar meson and of a vector meson [1]. To our knowledge, the present work is the first investigation in which the self-consistent Fock contribution is included. We focused on the prediction of this model concerning the average nucleon-nucleus potential, i.e. concerning the shell-model potential or more generally the real part of the optical-model potential. For this purpose, we constructed a Schroedinger-equivalent potential. The latter is a single-particle potential which when introduced in the non-relativistic Schroedinger equation yields the same bound state energies and the same elastic scattering phase shifts as the original relativistic single-particle potential did when used in conjunction with the Dirac equation. The comparison between this Schroedinger-equivalent potential and the central and spin-orbit components of the empirical optical-model potential is rather satisfactory provided that the coupling constants between the nucleon and the meson fields are suitably adjusted. This adjustment corresponds to the use of an effective meson-nucleon interaction [1,11]. One characteristic feature of the calculated Schroedinger-equivalent potential is that it has a "wine-bottle bottom" shape at intermediate energy ; in the present approach this shape is due to relativistic effects.

We hope that the relativistic Hartree-Fock model may become a workable and useful one if the experimental data are invoked to constrain the choice of the various meson-nucleon coupling constants. Here, we have put emphasis on the single-particle potential at low and intermediate energy. Other data should of course be considered. The most stringent restrictions will probably arise from those observables which involve the small components of the relativistic single-particle spinors [21, 22]. We believe that a relativistic approach will become not only of theoretical but also of practical interest if it is eventually confirmed that the relativistic single-particle potential involves several components which are comparable in magnitude to the nucleon rest mass.

FIGURE CAPTIONS

Fig. 1. Dependence upon the Fermi momentum k_F of the average binding energy per nucleon as calculated from the input parameter (18). The full curve corresponds to the Hartree approximation and the dashes to the Hartree-Fock approximation.

Fig. 2. Ratio between the baryon density ρ and the scalar density ρ_s, as calculated from Equations (13) with the input parameters (18).

Fig. 3. Adapted from ref. [7]. Comparison between the empirical (crosses, triangles, squares, dot) values of the volume integral per nucleon (25) and the theoretical value calculated from the self-consistent Hartree approximation with the input parameters (18), in the case of ^{40}Ca.

Fig. 4. Schroedinger-equivalent potential in the case of infinite nuclear matter with $k_F = 1.35$ fm^{-1} (full curve) and $k_F = 1.10$ fm^{-1} (dashed curve), in the case of the relativistic Hartree approximation with the input parameters (18).

Fig. 5. Adapted from ref. [7]. Schroedinger-equivalent potential as calculated from the relativistic Hartree approximation in the case of ^{40}Ca at $\epsilon = 163$ MeV.

Fig. 6. Adapted from ref. [7]. The dashed curve represents the real part of the optical-model potential determined by Elton [14] from the analysis of 180 MeV protons scattering by ^{56}Fe. The full curve shows the Schroedinger-equivalent potential as calculated from the relativistic Hartree approximation with the input parameter (18).

Fig. 7. Schroedinger-equivalent potential in the case of infinite nuclear matter with $k_F = 1.35$ fm^{-1} (full curve) and $k_F = 1.10$ fm^{-1} (dashed curve), in the case of the relativistic Hatree-Fock approximation with the input parameters (18).

REFERENCES

[1] J.D. WALECKA : Ann. of Phys. 83, 491 (1974).

[2] J.D. WALECKA : Nuclear Interactions, ed. B.A. Robson, (Springer-Verlag, 1978),p. 294 and references contained therein.

[3] B.D. SEROT and J.D. WALECKA : Phys. Lett. 87B, 172 (1979).

[4] L.D. MILLER and A.E.S. GREEN : Phys. Rev. C5, 241 (1972).

[5] R. BROCKMANN : Phys. Rev. C18, 1510 (1978).

[6] M. JAMINON, C. MAHAUX and P. ROCHUS : Phys. Rev. Lett. 43, 1097 (1979).

[7] M. JAMINON, C. MAHAUX and P. ROCHUS : Phys. Rev. (in press).

[8] S.A. CHIN : Ann. of Phys. 108, 301 (1977).

[9] L. WILETS : Mesons in Nuclei, ed. M. Rho and D.H. Wilkinson (North-Holland, Amsterdam 1979),p. 789.

[10] K. ERKELENZ, K. HOLINDE and R. MACHLEIDT : unpublished. See also K. HOLINDE, Nordita preprint 79/16.

[11] M.R. ANASTASIO, L.S. CELENZA and C.M. SHAKIN : preprint, May 1980.

[12] N.F. MOTT and H.S.W. MASSEY : The Theory of Atomic Collisions, 3rd edition (Clarendon Press, Oxford 1965), p. 228.

[13] A. INGEMARSSON : Physica Scripta 9, 156 (1974).

[14] L.R.B. ELTON : Nucl. Phys. 89, 69 (1966).

[15] B.C. CLARK : private communication (1980).

[16] H.O. MEYER, P. SCHWANDT, G.L. MOAKE and P.P. SINGH : preprint (1980).

[17] J.P. JEUKENNE, A. LEJEUNE and C. MAHAUX : Nuclear Self-Consistent Fields, ed. G. Ripka and M. Porneuf (North-Holland, Amsterdam 1975), p. 155.

[18] C. MAHAUX : Common Problems in Low-and Medium-Energy Nuclear Physics, ed. B. Castel (Plenum Press, 1979), p. 265.

[19] L.D. MILLER : Phys. Rev. C9, 537 (1974).

[20] M. BOLSTERLI : Phys. Rev. D11, 312 (1975).

[21] J.V. NOBLE : Phys. Rev. C20, 1188 (1979).

[22] J.M. EISENBERG : Tel-Aviv University preprint 871-80 (1980).

Figure 1.

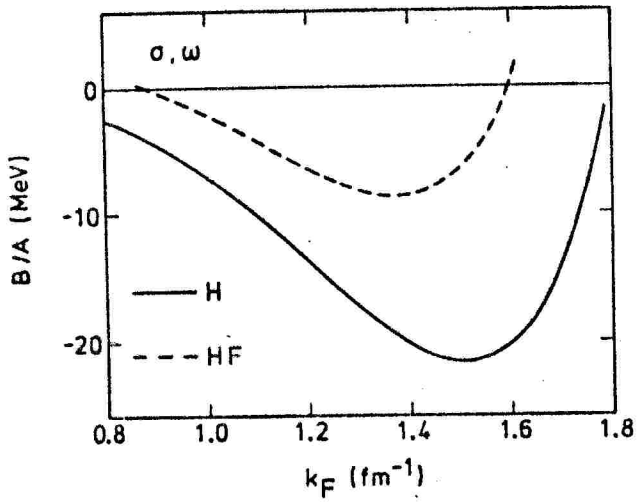

M. Jaminon et al. : "The shell-model..."

Figure 2.

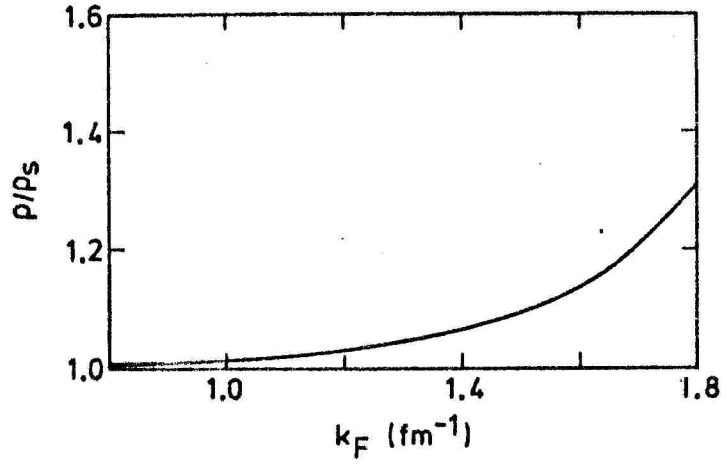

M. Jaminon et al. : "The shell-model..."

Figure 3.

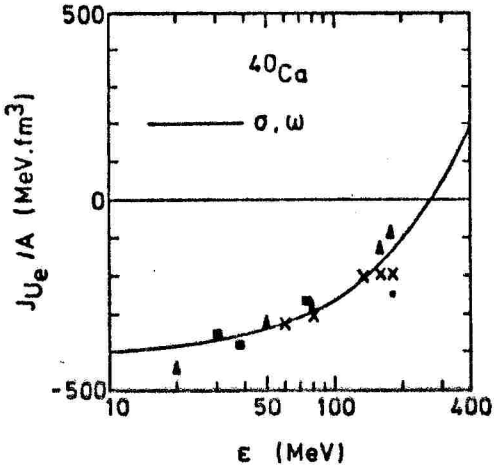

M. Jaminon et al. : "The shell-model..."

Figure 4.

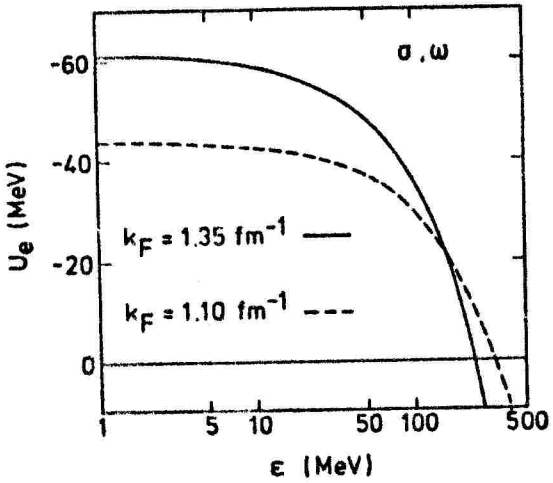

M. Jaminon et al. : "The shell-model..."

Figure 5.

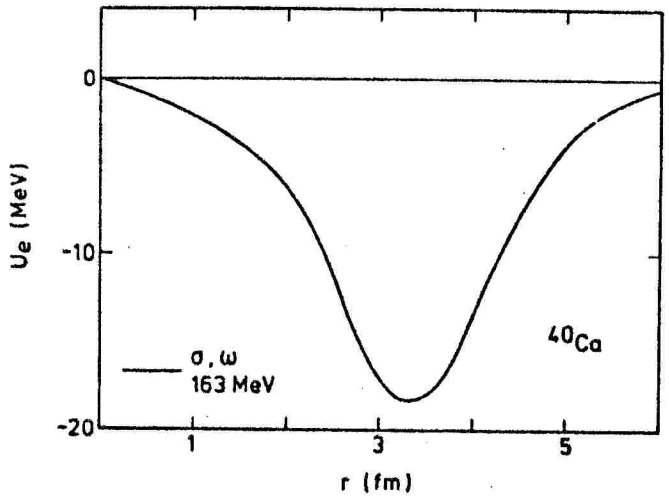

M. Jaminon et al. : "The shell-model..."

Figure 6.

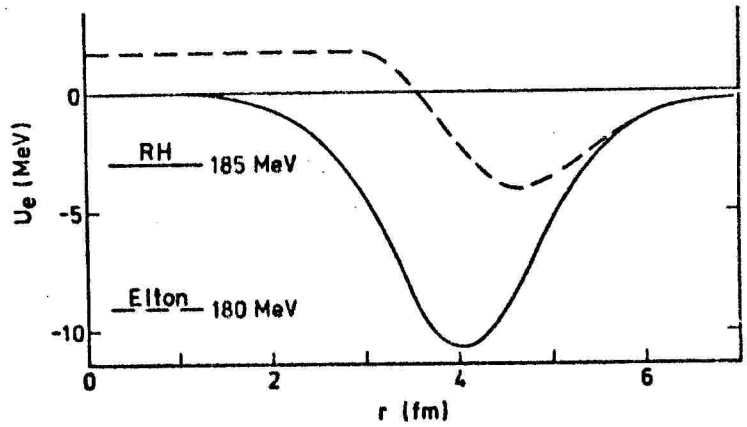

M. Jaminon et al. : "The shell-model..."

Figure 7.

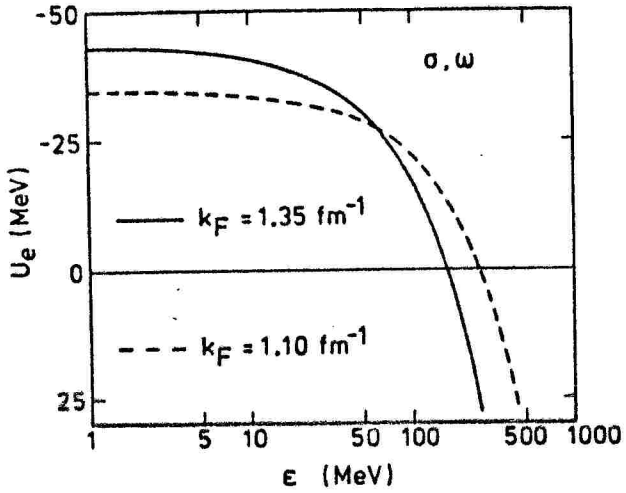
-50
-25
0
25
U_e (MeV)
σ, ω
k_F = 1.35 fm^{-1}
k_F = 1.10 fm^{-1}
1
5
10
50
100
500
1000
ε (MeV)